

Spin labelling via metabolic glycoengineering for studying post-translational protein modification by electron paramagnetic resonance spectroscopy

Received 00th January 20xx,
Accepted 00th January 20xx

DOI: 10.1039/x0xx00000x

Anna Rubailo,^a Valentin Wittmann^a and Malte Drescher^{*a}

^a University of Konstanz, Department of Chemistry and Konstanz Research School Chemical Biology, Konstanz, Germany

E-mail: malte.drescher@uni-konstanz.de

Post-translational modifications are involved in many cellular processes. The addition of O-linked β -N-acetylglucosamine (O-GlcNAc) is a ubiquitous post-translational modification and essential for regulatory processes in mammalian cells. Here, we demonstrate specific spin labelling of post-translational modifications, namely glycosylation modifications, via metabolic glycoengineering and subsequent copper-catalyzed azide-alkyne cycloaddition. Electron paramagnetic resonance spectroscopy and subsequent quantitative spectral simulations allow for detection of the labelled post-translational modifications.

Post-translational modifications (PTMs) of proteins are characterized by often reversible attachments of different chemical moieties ranging from small methyl groups via huge oligosaccharides to entire protein structures. A large number of human proteins associated with a variety of diseases incline for PTMs.^{1,2}

Only a limited number of experimental tools are available for studying PTMs. The majority of PTM detection methods has been developed to provide the best opportunity to identify, validate, and study the function of regulatory PTMs for a protein of interest.^{3,4} Most commonly, downstream methods like western blot or mass spectrometry are used to determine PTM patterns.⁵ However, not for all proteins site specific PTMs were identified.

Among the most important PTMs is glycosylation, characterized by complex and structurally diverse modification patterns resulting in a huge variety of glycosylation modifications of proteins.² O-GlcNAcylation, i.e. enzymatic addition of *N*-acetylglucosamine (GlcNAc) monosaccharide to specific Ser/Thr residues,⁶ regulates a wide variety of cellular functions including transcription, translation, and signal transduction in the cytosol, nucleus and mitochondria.^{6,7} O-GlcNAcylation is catalyzed by the O-linked *N*-acetylglucosaminyl transferase (OGT) and reverted by the enzyme O-GlcNAcase (OGA).^{8,9,10} Aberrant O-GlcNAcylation is highly related with chronic diseases. Dysregulation of O-GlcNAc modification leads to tumor growth and metastasis cancer processes and is provocative for metabolic disorders, cardiovascular disease, diabetes and Alzheimer's disease.¹¹

Metabolic glycoengineering (MGE) (also called metabolic oligosaccharide engineering (MOE))^{12,13} is an established method to incorporate chemical reporter groups into cellular glycans for subsequent bio-orthogonal labelling. MGE has found broad application for fluorescent labelling of carbohydrates, e.g. for visualization of glycans on the human cell surface¹⁴ or even within living cells.¹⁵ Also, global spin labelling of the layers of glycans on the cell surface called glycocalyx and subsequent electron paramagnetic resonance (EPR) measurements have been demonstrated.¹⁷ In addition, sialoglycans on the cell membrane were recently studied by EPR spectroscopy.¹⁸

Here, we set out to establish spin labelling of PTMs, namely protein glycosylation, via MGE to open the avenue for EPR experiments on specific target proteins modified in the cell.

As exemplary targets we choose two model proteins, mitochondrial O-linked *N*-acetylglucosaminyltransferase (mOGT) and cellular tumor antigen p53. Both were shown to feature O-GlcNAcylation in mammalian cells.¹⁰ mOGT, a variant of the OGT protein, consists of 1046 amino acids, has a molecular weight of 110 kDa, and forms a homodimer in its active state.¹⁸ p53 is a 393 amino acids protein with molecular weight of 44 kDa.¹⁹ For OGT the O-GlcNAc Database²⁰ reports seven O-GlcNAc sites. The list of O-GlcNAcylation sites in p53 and the effects of glycosylation on its function are still disputed.^{21, 22} Only one O-GlcNAc site is reported in the O-GlcNAc database for p53 (Ser149).²⁰ However, twelve phosphorylation sites are known for p53, and in case of incomplete phosphorylation these sites might also get glycosylated. Also, Yang *et al.* discuss Thr155 as O-linked glycosylation site for p53.²¹

The experimental strategy is shown in Figure 1. The target proteins, p53 or OGT, containing a His-tag for purification, were expressed in HEK 293T cells. We performed *in cellula* MGE to modify the target protein by tetraacetylated *N*-azidoacetyl-glucosamine (Ac₄GlcNAz) (see SI Fig. S1 (A)), which has previously been reported to be incorporated into O-GlcNAcylation proteins,²³ and used tetraacetylated *N*-acetylglucosamine (Ac₄GlcNAc) (SI Fig. S1 (B)) as negative control. After MGE, the target proteins were purified from the cell lysate by nickel-charged nitrilotriacetic acid (Ni-NTA) resin addressing the HIS tag (see SI, page 4). Upon protein purification, a nitroxide-based spin label (SL) was attached via copper-catalyzed [3+2] azide-alkyne cycloaddition (CuAAC) as an orthogonal click reaction directly on the Ni-NTA beads using an alkyne proxyl nitroxide radical²⁴ (Figure 2).

EPR spectra were measured in X band (9.47 GHz) at room temperature ($\approx 22^\circ\text{C}$) upon elution (elution details see SI page S5) to detect spin labelled glycosylation modifications and to monitor the SL dynamics. The EPR spectra (Figure 2) for OGT upon *in cellula* MGE with Ac₄GlcNAz and CuAAC spin labelling are typical nitroxide spectra featuring three lines due to hyperfine splitting. The spectrum of the negative control, OGT upon *in cellula* MGE with Ac₄GlcNAc, does not show any EPR signal above the detection limit (Figure 2B, red). Therefore, we conclude that Ac₄GlcNAz spin labelling of modified OGT does take place selectively at the azido groups.

For the OGT sample modified with Ac₄GlcNAz, upon elution, buffer exchange and concentrating the protein solution to the original volume, we find a spin concentration of 0.87 μM at a protein concentration of 266 μM corresponding to a relative spin concentration of approximately 0.3% per molecule.

Similar experiments were performed for p53, which is skewed-cube-shaped prone.²⁵ The corresponding EPR spectra are shown in Figure 3. Despite the low spin concentration (0.14 μM at a protein concentration of 30 μM , corresponding to 0.5%), an EPR signal was detected for the sample modified with Ac₄GlcNAz, but not for the negative control.

The relative spin concentrations reflect i) the glycosylation statistics including the competition between the artificial GlcNAz and the

native GlcNAc sugars, and ii) the spin labelling efficiency in the CuAAC reaction.

In a control experiment under similar conditions, we determined the spin labelling efficiency of Ac₄GlcNAz with alkyne-proxyl in the CuAAC reaction to approximately 75% (see SI Fig.5 B), which is in agreement with formerly reported CuAAC spin labelling efficiencies.^{24,26} Assuming a labelling efficiency of 75% for the metabolically incorporated Ac₄GlcNAz, we estimate a relative O-GlcNAz level of 0.4% (0.6%) per protein OGT (p53).

To analyze the SL dynamics, we performed full spectral simulations for the EPR spectra (Figure 4). A) SL in solution, B) SL attached to Ac₄GlcNAz in solution, C) SL attached to GlcNAz incorporated in OGT and D) SL attached to GlcNAz incorporated in p53. Spectral simulations were performed using the toolbox EasySpin 5.2.29.²⁷ assuming an isotropic rotation of SL and only varying the rotational correlation time between the different spectra (parameters described in SI).

While the model of isotropic tumbling for the cases A) and B) worked well for describing the corresponding EPR spectra, the isotropic tumbling fits for SL attached to the proteins (C, D) are – as expected – slightly oversimplified but the isotropic rotational correlation time τ_r can be used as semi-empirical parameter. Note that besides possible partially anisotropic tumbling, the spectra might be obtained for several labelled sites within the protein. As every site might be characterized by somewhat different SL dynamics, a combination of such sites might appear to not fit perfectly to a single τ_r approximation, even if the tumbling at each site is approximately isotropic. The spectra were best described by the rotational correlation times of $\tau_r = 10$ ps for the free SL, $\tau_r = 79$ ps for the free label attached to the sugar Ac₄GlcNAz, $\tau_r = 1.0$ ns, and $\tau_r = 1.2$ ns for the spin label attached to OGT or p53. The increase of τ_r with increasing complex size, i.e. from A) over B) to C) or D), respectively, reflects the slower tumbling of SL. In cases C) and D), τ_r does not reflect the overall molecular tumbling of the complex but rather the flexibility of the secondary structure element involved or steric hindrance from inter- and intra-molecular interactions.²⁸ Since p53 is prone to tetramerisation,²⁵ this might result in slightly slower tumbling of SL in p53 as compared to OGT.

In summary, we have demonstrated that spin labels can be attached to post translationally glycosylated sites of proteins of interest employing MGE. This approach combines *in cellula* MGE with bio-orthogonal spin labelling reaction and provides a facile technology to probe protein O-GlcNAc modification by EPR spectroscopy.

In future, the spin labelling approach can potentially be transferred into cells.^{24,26} Also obtaining distance restraints in the nanometer range²⁹⁻³⁴ might be feasible.

Acknowledgements

This work was supported by DAAD (Deutscher Akademischer Austauschdienst/German Academic Exchange Service) and has received funding from the European Research Council (ERC) under the European Union's Horizon 2020 research and innovation programme (grant agreement no. 772027-SPICE-ERC-2017-COG) and the Deutsche Forschungsgemeinschaft (SFB 969, project B05).

Experimental details

DNA plasmid of OGT/O-linked N-acetylglucosamine transferase gene ORF cDNA clone expression plasmid, N-His tag (from Biozol, Artikel-Nr. SIN-HG17892-NH-1) and p53_{WT}-His in pcDNA3.1 were used for

the HEK 293T human cell line expression. O-linked modification of the expressed proteins were performed via metabolic glycoengineering (MGE). O-GlcNAcylated protein was obtained after harvesting the cells and purified on the Ni-NTA resin. Spin labelling was performed both on resin-bound protein and after elution.

X-band (9.47 GHz) CW EPR measurements were performed on a Bruker EMXnano. Spectra for each sample were acquired at optimal modulation amplitude and microwave power to avoid over-modulation and saturation, respectively. Each individual sample of proteins was prepared by purification from lysate of HEK 293T cell culture previously treated with Ac₄GlcNAz, and purified from the cells lysate. EPR measurements were performed with 50 μ l samples in capillaries (HIRSCHMANN® ringcaps®; inner diameter 1.02 mm). All measurements were performed at 22 °C.

For the quantitative EPR spectral simulations Matlab R2019b (The MathWorks, Inc. 3 Apple Hill Drive, Natick, MA 01760-2098, USA) and EasySpin 5.2.29 toolbox were used.^{24,27} The EPR base line correction was performed with a second order polynomial function. CW-EPR spectra in fast motion regime were simulated with the EasySpin function *chilli*. Least-squares fits with varying simulation parameters to the experimental data was performed using EasySpin fitting function *esfit*.^{22,26}

Detailed protocols can be found in SI.

Conflicts of interest

There are no conflicts to declare.

Notes and references

1. A. M. Bode, Z. Dong, Post-translational modification of p53 in tumorigenesis // *Nature Reviews Cancer*, 2004, 4(10), 793-805.
2. A. Varki, R. D. Cummings, J. D. Esko, P. Stanley, G. W. Hart, M. Aebi, A. G. Darvill, T. Kinoshita, N. H. Packer, J. H. Prestegard, R. L. Schnaar and P. H. Seeberger, eds., *Essentials of Glycobiology*, Cold Spring Harbor Laboratory Press, Cold Spring Harbor, NY, 2015-2017.
3. L. Bonilla, G. Means, K. Lee, S. Patterson. *Biotechniques*. 2008; 44(5), 671–9.
4. S. Sigismund, V. Algisi, G. Nappo, A. Conte, R. Pascolutti, A. Cuomo, T. Bonaldi, E. Argenzio, LG. Verhoef, E. Maspero, et al. *EMBO J.*, 2013, **32(15)**, 2140-57.
5. CL. Li, A. Sathyamurthy, A. Oldenborg, D. TankJ *Neurosci*. 2014, **34(11)**, 4027–42.
6. S. Hardivillé and G. W. Hart, *Cell Metab.*, 2014, **20**, 208–213.
7. G. W. Hart, C. Slawson, G. Ramirez-Correa, O. Lagerlof, *Annu Rev Biochem*. 2011, **80**, 825–858.
8. M. R. Bond and J. A. Hanover, *J. Cell Biol.*, 2015, **208**, 869–880.
9. G. W. Hart, M. P. Housley, C. Slawson, *Nature.*, 2007, **446**, 1017–22.
10. X. Yang, K. Qian, *Nat Rev Mol Cell Biol*, 2017, **18(7)**, 452-465.
11. Y. R. Yang, P. G. Suh, O-GlcNAcylation in cellular functions and human diseases // *Advances in biological regulation*. – 2014. – T. 54. – C. 68-73.
12. O. T. Keppler, R. Horstkorte, M. Pawlita, C. Schmidt and W. Reutter, *Glycobiology*, 2001, **11**, 11R-18R.
13. D. H. Dube and C. R. Bertozzi, *Curr. Opin. Chem. Biol.*, 2003, **7**, 616-625.
14. P. R. Wratil, R. Horstkorte and W. Reutter, *Angew. Chem., Int. Ed.*, 2016, **55**, 9482-9512; K. K. Palaniappan and C. R. Bertozzi, *Chem. Rev.*, 2016, **116**, 14277-14306; T. J. Sminia, H. Zuilhof and T. Wennekes, *Carbohydr. Res.*, 2016, **435**, 121-141; P. A. Gilormini, A. R. Batt, M. R. Pratt and C. Biot, *Chem. Sci.*, 2018, **9**, 7585-7595; C. Agatemor, M. J. Buettner, R. Ariss, K. Muthiah, C. T. Saeui and K. J.

- Yarema, *Nat. Rev. Chem.*, 2019, **3**, 605-620; L. M. Haiber, M. Kufleitner and V. Wittmann, *Front. Chem.*, 2021, **9**, 654932.
15. F. Doll, A. Buntz, A.-K. Späte, V. F. Schart, A. Timper, W. Schrimpf, C. R. Hauck, A. Zumbusch and V. Wittmann, *Angew. Chem., Int. Ed.*, 2016, **55**, 2262–2266; F. Doll, J. Hassenrück, V. Wittmann and A. Zumbusch, *Methods Enzymol.*, 2018, **598**, 283-319.
16. M. Jaiswal, T. T. Tran, Q. Li, X. Yan, M. Zhou, K. Kundu and Z. Guo, *Chemical Science*, 2020, **11(46)**, 12522-12532.
17. M. Jaiswal, T. T. Tran, J. Guo, M. Zhou, J. G. Diaz, G. E. Fanucci and Z. Guo, *Analyst.* – 2022, **147**, 784-788.
18. C. Butkinaree, K. Park and G. W. Hart, *Biochimica et biophysica acta*, 2010, 1800(2), 96-106.
19. G. Chillemi, S. Kehroesser, F. Bernassola, A. Desideri, V. Dötsch, A. J. Levine, G. Melino, *Cold Spring Harb Perspect Med.*, 2017, **7(4)**, a028308.
20. E. Wulff-Fuentes, R. R. Berendt, L. Massman, L. Danner, F. Malard, J. Vora, R. Kahsay, S. Olivier-Van Stichelen, *The Human O-GlcNAcome Database and Meta-Analysis. Scientific Data*, 2021; **8(1)**:25.
21. W. H. Yang, J. E. Kim, H. W. Nam, J. W. Ju, H. S. Kim, Y. S. Kim, & J. W. Cho, *Nature cell biology*, 2006, **8(10)**, 1074-1083.
22. R. M. de Queiroz, R. Madan, J. Chien, W. B. Dias, C. Slawson, *J Biol Chem.*, 2016 Sep 2, **291(36)**, 18897-914.
23. D. J. Vocadlo, H. C. Hang, E.-J. Kim, J. A. Hanover and C. R. Bertozzi, *Proc. Natl. Acad. Sci. U. S. A.*, 2003, **100**, 9116-9121.
24. S. Kucher, S. Korneev, S. Tyagi, R. Apfelbaum, D. Grohmann, E. A. Lemke, J. P. Klare, H. J. Steinhoff and D. Klose, *J. Magn. Reson.*, 2017, **275**, 38 – 45.
25. A. L. Okorokov, M. B. Sherman, C. Plisson, V. Grinkevich, K. Sigmundsson, G. Selivanova, & E. V. Orlova, 2006, **25(21)**, 5191–5200.
26. P. Widder, J. Schuck, D. Summerer and M. Drescher, *Phys. Chem. Chem. Phys.*, 2020, **22**, 4875-4879.
27. S. Stoll and A. Schweiger, *Journal of magnetic resonance*, 2016, **178(1)**, 42-55.
28. E. Bordignon, *EPR spectroscopy of nitroxide spin probes //EPR Spectroscopy: Fundamentals and Methods.* – John Wiley, 2018, 277.
29. S. Stoll *Methods in Enzymology*, 2015, **563**, 121 – 142.
30. J. Janetzko, S. Walker, *J Biol Chem.*, 2014, **289**, 34424
31. G. Jeschke, *Protein Science*, 2018, **27**, 76–85
32. G. Jeschke, *Annu. Rev. Phys. Chem.*, 2012, **63**, 419–446.
33. M. Pannier, S. Veit, A. Godt, G. Jeschke, H. W. Spiess, *J. Magn. Reson.*, 2000, **142**, 331–340.
34. T. Prisner, M. Rohrer & F. MacMillan, 2001, **52(1)**, 279 – 313.

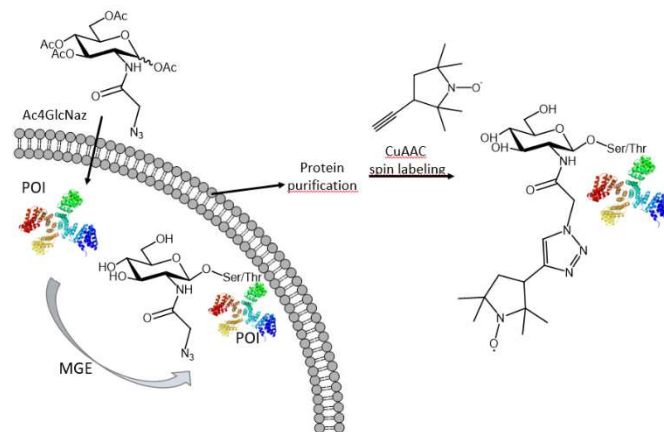


Fig. 1 Schematic representation of the experimental strategy. The target protein (here: OGT) is expressed in HEK293T cells. Ac₄GlcNAz is transfected into the cell, deacetylated, and converted to GlcNAz for the further metabolic pathway. After MGE and protein purification, the attached azido sugar was selectively labelled via Copper click chemistry with Alkyne Proxyl spin label for EPR investigation.

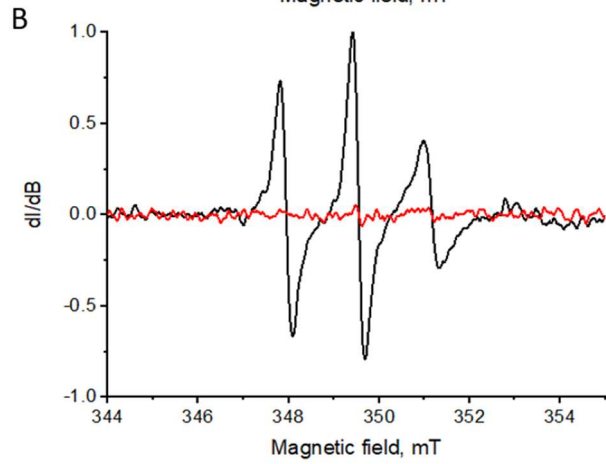
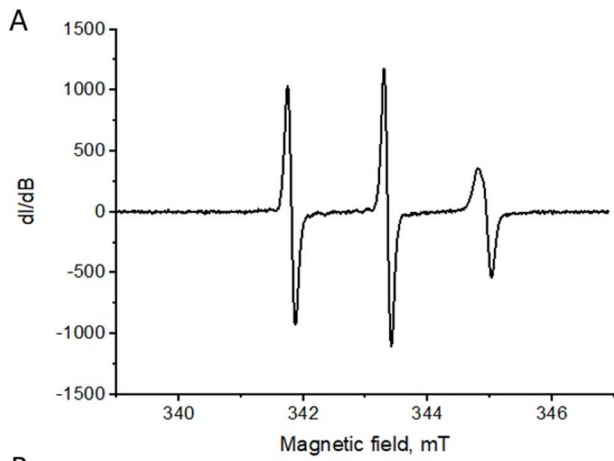


Fig. 2 X-band EPR spectra of (A) OGT protein upon in vivo MGE with $Ac_4GlcNAz$ and CuAAC spin labelling attached to the Ni-beads via His-tag and subsequent elution (B) OGT protein upon in vivo MGE with $Ac_4GlcNAz$ and CuAAC spin labelling after elution from purified Ni-beads (black curve); negative control: OGT protein upon in vivo MGE with $Ac_4GlcNAc$ and CuAAC spin labelling after elution from purified Ni-beads (red curve). All samples were prepared with the same amount of expressed HEK 293T cells.

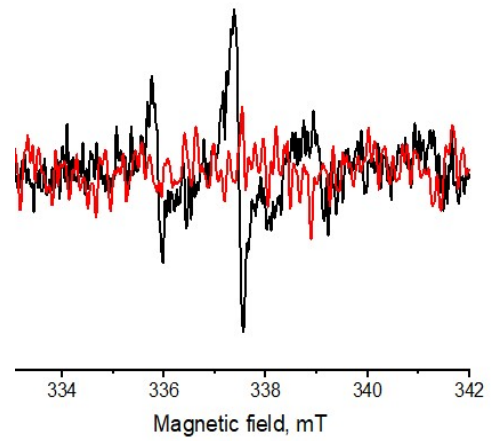


Fig. 3 X-band EPR spectra of p53 upon in vivo MGE with $Ac_4GlcNAz$ and CuAAC spin labelling on Ni-beads via His-tag and subsequent elution (black curve). Red: negative control using ($Ac_4GlcNAc$) without an azido group (red curve).

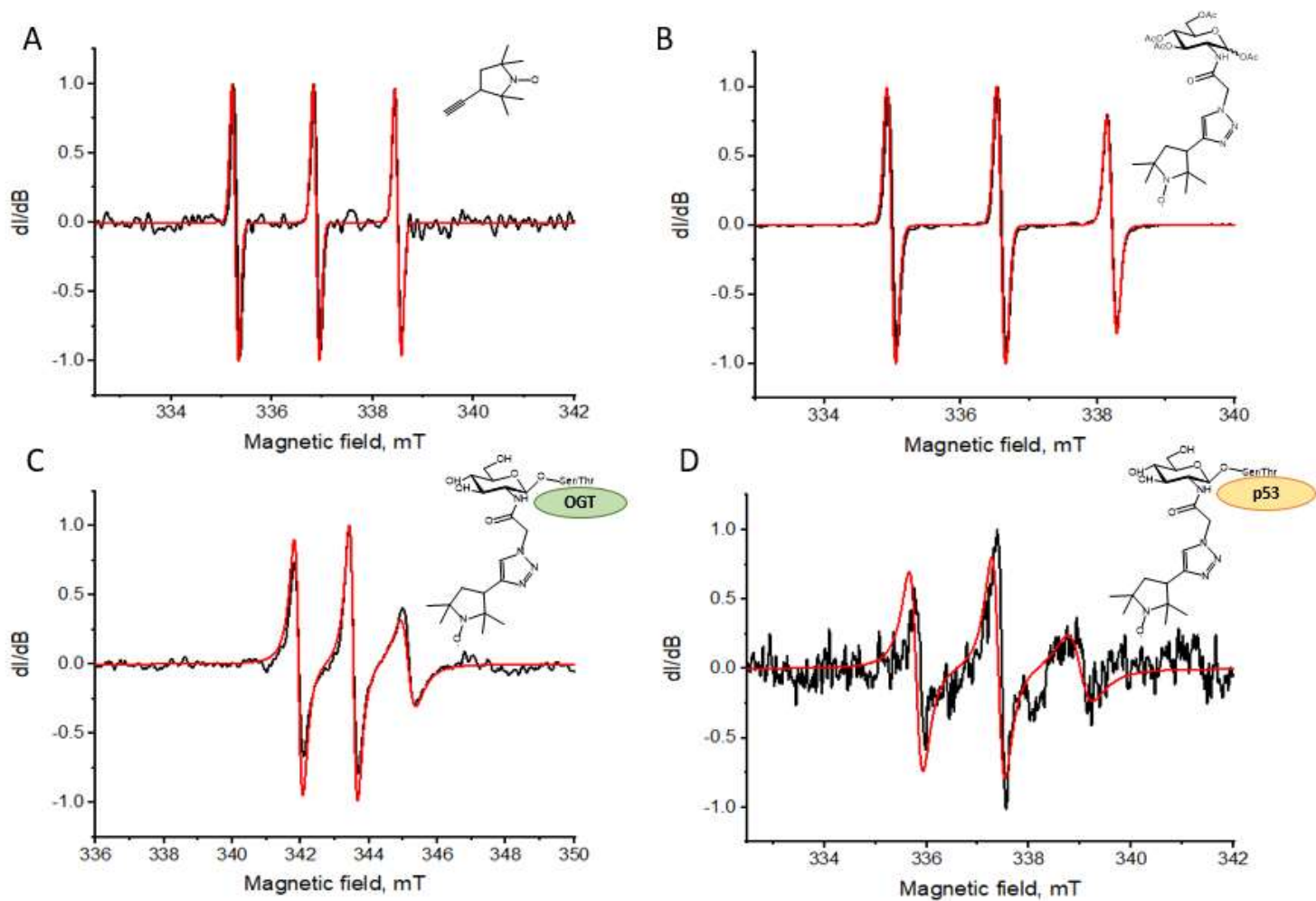


Fig. 4 Experimental EPR spectra (black) and full spectral simulations (red) for (A) SL in solution ($\tau_r = 10.23$ ps), (B) SL attached to $Ac_4GlcNAz$ in solution ($\tau_r = 79$ ps), (C) SL attached to GlcNAz incorporated in OGT ($\tau_r = 1.00$ ns) and (D) SL attached to GlcNAz incorporated in p53 ($\tau_r = 1.2$ ns).